

Predictions from High Scale Mixing Unification Hypothesis

Gauhar Abbas,^{1,*} Saurabh Gupta,^{1,†} G. Rajasekaran,^{1,2,‡} and Rahul Srivastava^{1,§}

¹*The Institute of Mathematical Sciences, Chennai 600 113, India*

²*Chennai Mathematical Institute, Siruseri 603 103, India*

We investigate the renormalization group evolution of masses and mixing angles of Majorana neutrinos under the ‘High Scale Mixing Unification’ hypothesis. Assuming the unification of quark-lepton mixing angles at a high scale, we show that all the experimentally observed neutrino oscillation parameters can be obtained, within $3\text{-}\sigma$ range, through the running of corresponding renormalization group equations provided neutrinos have same CP parity and are quasi-degenerate. One of the novel results of our analysis is that θ_{23} turns out to be non-maximal and lies in the second octant. Furthermore, we derive new constraints on the allowed parameter space for the unification scale, SUSY breaking scale and $\tan\beta$, for which the ‘High Scale Mixing Unification’ hypothesis works.

PACS numbers: 14.60.Pq, 11.10.Hi, 11.30.Hv, 12.15.Lk

I. INTRODUCTION

The quest for a unified theory of quarks and leptons is one of the main goals of beyond standard model physics. To this end, the unification of mixing angles of quarks and leptons, at a high scale, seems to be an exciting possibility. In the past, it has been investigated under the hypothesis referred to as ‘High Scale Mixing Unification’ (HSMU) for the case of Majorana neutrinos [1–5] and, recently, for the case of Dirac neutrinos [6]. A similar possibility has also been investigated in [7]. Within the HSMU hypothesis, the observed values of oscillation parameters at low energies are obtained through the renormalization

*Electronic address: gauhar@imsc.res.in

†Electronic address: saurabh@imsc.res.in

‡Electronic address: graj@imsc.res.in

§Electronic address: rahuls@imsc.res.in

group (RG) evolution of these parameters from the unification scale (high scale) to the low scale M_Z (mass of the Z boson).

In addition, the HSMU hypothesis also provides hints about the type and nature of the underlying unified theory that might exist at the unification scale. One of the key predictions of the HSMU hypothesis is the small non-zero value of θ_{13} [1–5]. At the time of the earlier work on HSMU, only an upper bound on θ_{13} existed and it was not known whether θ_{13} was zero or non-zero.

The recent results from different experiments have established the value of θ_{13} to be non-zero [8–12]. This precise measurement can be used to test predictions of various models and put stringent constraints on them. The current global scenario of the neutrino oscillation parameters (for normal hierarchy pattern) [13, 14] is summarized in the Table I. Since θ_{13} is fairly well determined now, it is important to check whether HSMU is consistent with this measurement.

Quantity	Best Fit $\pm 1\text{-}\sigma$	$3\text{-}\sigma$ Range
Δm_{21}^2 (10^{-5} eV ²)	$7.50^{+0.18}_{-0.19}$	7.00 – 8.09
Δm_{31}^2 (10^{-3} eV ²)	$2.473^{+0.070}_{-0.067}$	2.276 – 2.695
$\theta_{12}/^\circ$	$33.36^{+0.81}_{-0.78}$	31.09– 35.89
$\theta_{23}/^\circ$	$40.0^{+2.1}_{-1.5} \oplus 50.4^{+1.3}_{-1.3}$	35.8 – 54.8
$\theta_{13}/^\circ$	$8.66^{+0.44}_{-0.46}$	7.19 – 9.96

TABLE I: The global fits for neutrino oscillation parameters [14].

Furthermore, with the operation of the Large Hadron Collider (LHC), two important developments have occurred. What is presumably the long awaited Higgs boson has been discovered with a mass around 125 GeV [15, 16] and so far, no signature of supersymmetry (SUSY) has been observed [17–19]. Both of these, especially the second one, can have important repercussions on the implementation of HSMU.

In the earlier works on HSMU hypothesis, the issue of variation of SUSY breaking scale as a function of $\tan \beta$ was explored in the split SUSY scenario [4]. In the present work, we derive new constraints on the allowed ranges of SUSY breaking scale and $\tan \beta$ in the case of Minimal Supersymmetric Standard Model (MSSM). It was also shown that this hypothesis works for a wide range of unification scales [1]. We investigate it further and derive new

constraints on the variation of unification scale. In view of the availability of more precise values of the neutrino oscillation parameters [13, 14] these investigations are likely to serve as important tests of HSMU hypothesis. A detailed discussion of these constraints is one of the main features of this paper.

This paper is organized in the following manner. In section II, we provide a general formalism of the RG running of Majorana neutrino masses and mixing angles. Section III, contains our results for the neutrino oscillation parameters at low energy within the framework of HSMU hypothesis. In section IV, we discuss various predictions originating from our analysis. The constraints on the unification scale, SUSY breaking scale and $\tan\beta$ are derived in section V. Finally, in section VI, we summarize our results and give future directions.

II. RENORMALIZATION GROUP EVOLUTION OF NEUTRINO MASSES AND MIXING ANGLES

We present, in this section, the RG equations used in our analysis. Our basic assumption is that the neutrinos are Majorana type and mass eigenstates m_i , ($i = 1, 2, 3$) are of same CP parity. We also ignore CP violating phases in the mixing matrix. With these assumptions, the real PMNS matrix can be parametrized as

$$U = \begin{bmatrix} c_{12}c_{13} & s_{12}c_{13} & s_{13} \\ -s_{12}c_{23} - c_{12}s_{23}s_{13} & c_{12}c_{23} - s_{12}s_{23}s_{13} & s_{23}c_{13} \\ s_{12}s_{23} - c_{12}c_{23}s_{13} & -c_{12}s_{23} - s_{12}c_{23}s_{13} & c_{23}c_{13} \end{bmatrix}, \quad (1)$$

with $c_{ij} = \cos\theta_{ij}$ and $s_{ij} = \sin\theta_{ij}$ ($i, j = 1, 2, 3$). The U matrix diagonalizes the neutrino mass matrix M in the flavor basis, i.e. $U^T M U = \text{diag}(m_1, m_2, m_3)$.

Here, we take a model independent approach and assume that the new physics operating at the unification scale results in the unification between CKM and PMNS mixing angles. In order to get the low scale values, we work in type-I seesaw scenario. For the RG running from unification scale to seesaw scale, we use the standard MSSM RG equations within the framework of type-I seesaw mechanism [20]. Below the seesaw scale all right handed neutrinos are integrated out and the masses of left handed neutrinos are generated by a dimension 5 operator added to the standard SM/MSSM Lagrangian. We have numerically

checked our results by varying seesaw scale from $10^{13} - 10^9$ GeV and we find that our analysis depends weakly on the chosen value of seesaw scale. Thus, for the sake of illustration and definiteness, we have taken seesaw scale of $\mathcal{O}(10^{10})$ GeV throughout this work.

At this juncture, we would like to point out that, for our analysis, we do not need any details of the theory operating at the unification scale. Although one such high energy theory has already been discussed in literature (see, e.g. [1] for details). Moreover, RG equations presented here are at one loop level and only dominant terms are shown (cf. (2) and (5) below). However, in numerical computations, we have used full two-loop RG equations [21].

The RG evolution of neutrino masses m_i , below seesaw scale, is determined by the following equations [20–23]

$$\frac{dm_i}{dt} = \frac{m_i}{16\pi^2} [\alpha + C f_\tau^2 F_i] , \quad (2)$$

where $t = \ln(\mu/\mu_0)$, μ is the renormalization scale and F_i (with $i = 1, 2, 3$) are defined as

$$\begin{aligned} F_1 &= 2s_{12}^2 s_{23}^2 - s_{13} \sin 2\theta_{12} \sin 2\theta_{23} + 2s_{13}^2 c_{12}^2 c_{23}^2 , \\ F_2 &= 2c_{12}^2 s_{23}^2 + s_{13} \sin 2\theta_{12} \sin 2\theta_{23} + 2s_{13}^2 s_{12}^2 c_{23}^2 , \\ F_3 &= 2c_{13}^2 c_{23}^2 . \end{aligned} \quad (3)$$

In SM and MSSM, α , f_τ and C are

$$\begin{aligned} \alpha_{\text{MSSM}} &= -\frac{6}{5}g_1^2 - 6g_2^2 + \frac{6y_t^2}{\sin^2 \beta} , \\ \alpha_{\text{SM}} &= -3g_2^2 + 2y_\tau^2 + 6(y_t^2 + y_b^2) + \lambda , \\ f_{\tau, \text{MSSM}}^2 &= \frac{y_\tau^2}{\cos^2 \beta} , \quad f_{\tau, \text{SM}}^2 = y_\tau^2 , \\ C &= 1 \quad \text{in MSSM} , \quad C = -\frac{3}{2} \quad \text{in SM} . \end{aligned} \quad (4)$$

Here y_f , ($f = \tau, t, b$) represents the Yukawa coupling for τ -lepton, top and bottom quarks, respectively. The gauge couplings are denoted by g_i and λ stands for the Higgs self-coupling in SM.

The RG equations which govern evolution of mixing angles are given as [20–23]

$$\begin{aligned} \frac{d\theta_{12}}{dt} &= -\frac{C f_\tau^2}{32\pi^2} \sin 2\theta_{12} s_{23}^2 \frac{(m_1 + m_2)^2}{\Delta m_{21}^2} + \mathcal{O}(\theta_{13}), \\ \frac{d\theta_{13}}{dt} &= -\frac{C f_\tau^2}{32\pi^2} \sin 2\theta_{12} \sin 2\theta_{23} \frac{m_3}{\Delta m_{32}^2 (1 + \xi)} [(m_2 - m_1) + \xi (m_2 + m_3)] + \mathcal{O}(\theta_{13}), \\ \frac{d\theta_{23}}{dt} &= -\frac{C f_\tau^2}{32\pi^2} \sin 2\theta_{23} \frac{1}{\Delta m_{32}^2} \left[c_{12}^2 (m_2 + m_3)^2 + s_{12}^2 \frac{(m_1 + m_3)^2}{1 + \xi} \right] + \mathcal{O}(\theta_{13}), \end{aligned} \quad (5)$$

with

$$\xi = \frac{\Delta m_{21}^2}{\Delta m_{32}^2}, \quad \Delta m_{21}^2 = m_2^2 - m_1^2, \quad \Delta m_{32}^2 = m_3^2 - m_2^2. \quad (6)$$

In this work, Dirac as well as Majorana phases of the PMNS mixing matrix are taken to be zero. The results with non-zero phases will be presented in a future publication [24]. In (2) and (5), for sake of brevity, we have given only the dominant terms of the RG equations at one loop level. The full two loop RG equations, used in this work, can be found in [21]. The numerical computations, at two loop, are done using a MATHEMATICA based package REAP [20].

III. MAGNIFICATION OF MIXING ANGLES VIA RG EVOLUTION

The HSMU hypothesis is implemented in two steps. We first follow a bottom-up approach and take the known values of gauge couplings, Yukawa couplings and CKM matrix elements at the low scale (M_Z) [25] and evolve them up to the SUSY breaking scale (M_{SUSY}) using the standard SM RG equations [23]. From the SUSY breaking scale to the unification scale, the evolution of these parameters is governed by MSSM RG equations [21, 23].

At the unification scale, following the HSMU hypothesis, we assume that the PMNS mixing angles ($\theta_{12}^0, \theta_{13}^0, \theta_{23}^0$) are identical to the CKM mixing angles ($\theta_{12}^{0,q}, \theta_{13}^{0,q}, \theta_{23}^{0,q}$). In addition to this, we choose initial neutrino masses to be quasi-degenerate with normal hierarchy pattern and PMNS phases to be zero. The requirements of normal hierarchy and quasi-degeneracy of neutrinos are essential ingredients to achieve large mixing angle magnification (within the $3\text{-}\sigma$ range at the low scale) [1].

We then follow a top-down approach and run down the neutrino masses and mixing angles from unification scale to the seesaw scale using MSSM RG equations within the framework of type-I seesaw mechanism [20]. From seesaw scale to SUSY breaking scale, the running is done using MSSM RG equations with dimension-5 operator [21, 23]. Below the SUSY breaking scale to the low scale, RG running is governed by the SM RG equations.

In the earlier works on HSMU hypothesis [1–5], the SUSY breaking scale was taken as 1 TeV. At present, this is not favored by direct SUSY searches at the LHC [17, 18]. In view of this, we have taken the SUSY breaking scale as 2 TeV. The working of HSMU hypothesis requires large values of $\tan\beta$ which is also consistent with constraints imposed

by SUSY searches [18, 19, 26–28]. Therefore, in this section, we have taken $\tan\beta$ to be 55. Moreover, we have taken unification scale to be 2×10^{16} GeV which is a generic scale for Grand Unified Theories (GUTs). The dependence of our analysis on these parameters is discussed in section V.

TABLE II: Radiative magnification to bilarge mixings at low energies for input values of $\theta_{12}^0 = \theta_{12}^{0,q} = 13.02^0$, $\theta_{23}^0 = \theta_{23}^{0,q} = 2.03^0$ and $\theta_{13}^0 = \theta_{13}^{0,q} = 0.17^0$. We have taken the unification scale $= 2 \times 10^{16}$ GeV, $M_{SUSY} = 2$ TeV and $\tan\beta = 55$. The various entries in the table also highlight the correlations between low scale neutrino oscillation parameters.

	I	II	III	IV	V
$m_1^0(\text{eV})$	0.4152	0.3972	0.4344	0.4102	0.4240
$m_2^0(\text{eV})$	0.4186	0.4005	0.4380	0.4137	0.4275
$m_3^0(\text{eV})$	0.4825	0.4617	0.5049	0.4769	0.4928
$m_1(\text{eV})$	0.3577	0.3422	0.3742	0.3534	0.3653
$m_2(\text{eV})$	0.3583	0.3428	0.3749	0.3541	0.3659
$m_3(\text{eV})$	0.3620	0.3463	0.3788	0.3578	0.3697
$\Delta m_{21}^2(\text{eV}^2)_{RG}$	4.29×10^{-4}	3.93×10^{-4}	4.70×10^{-4}	4.49×10^{-4}	4.20×10^{-4}
$\Delta m_{32}^2(\text{eV}^2)_{RG}$	2.67×10^{-3}	2.45×10^{-3}	2.92×10^{-3}	2.61×10^{-3}	2.78×10^{-3}
$M_{\bar{e}}/M_{\bar{\mu},\bar{\tau}}$	1.85	1.81	1.89	1.76	2.06
$\Delta m_{21}^2(\text{eV}^2)_{th}$	-3.54×10^{-4}	-3.12×10^{-4}	-4.00×10^{-4}	-3.73×10^{-4}	-3.44×10^{-4}
$\Delta m_{32}^2(\text{eV}^2)_{th}$	-2.74×10^{-4}	-2.41×10^{-4}	-3.09×10^{-4}	-2.16×10^{-4}	-3.81×10^{-4}
$\Delta m_{21}^2(\text{eV}^2)$	7.52×10^{-5}	8.07×10^{-5}	7.02×10^{-5}	7.57×10^{-5}	7.56×10^{-5}
$\Delta m_{32}^2(\text{eV}^2)$	2.40×10^{-3}	2.20×10^{-3}	2.62×10^{-3}	2.40×10^{-3}	2.40×10^{-3}
$\theta_{23}/^\circ$	54.00	54.00	54.00	53.84	54.10
$\theta_{13}/^\circ$	8.67	8.67	8.67	8.66	8.66
$\theta_{12}/^\circ$	33.38	33.38	33.38	31.14	35.87

In Table II, we present five sets of neutrino oscillation parameters at low and high energy scales obtained within HSMU hypothesis. Each column in the table depicts some specific set of values for neutrino oscillation parameters chosen in a way to show correlations between them. In order to highlight the correlation between any two low scale parameters we choose

the unification scale neutrino masses such that all other parameters, at the low scale, remain close to their best fit values¹. In column I, all the low scale parameters are obtained close to their best fit values, except θ_{23} which is 54° . In column II, keeping θ_{13} and θ_{12} close to their best fit values at the low scale, the values of Δm_{21}^2 and Δm_{32}^2 are obtained at their $3\text{-}\sigma$ upper and lower edge respectively. For this pattern, θ_{23} again turns out to be 54° , i.e. non-maximal. Whereas, in column III, Δm_{21}^2 and Δm_{32}^2 are respectively kept at their $3\text{-}\sigma$ lower and upper edge. The rest of the results are similar to the previous ones. In columns IV and V, θ_{12} is taken to its lower and upper $3\text{-}\sigma$ limit, respectively, keeping all other parameters (except θ_{23}) close to their best fit values at the low scale. We see that θ_{23} always remains above 45° and lies in the second octant. Moreover, as is clear from Table II, for a fixed value of θ_{13} , the correlation between θ_{12} and θ_{23} is weak.

The RG evolution of the three PMNS and CKM mixing angles from the unification scale (2×10^{16} GeV) to the low scale (M_Z) is shown in Figure 1. As clear from the figure, owing to the quasi-degeneracy of neutrino masses, large angle magnification occurs in the PMNS sector. The magnification of CKM mixing angles (θ_{ij}^q , $i, j = 1, 2, 3$) is almost negligible because of the hierarchical nature of quark masses. We also observe that the major part of magnification occurs near SUSY breaking scale which, in this case, is chosen to be $M_{SUSY} = 2 \times 10^3$ GeV. The SM RG equations lead to negligible angle magnification as clear from the flatness of curves below M_{SUSY} .

The RG evolution of neutrino masses from unification scale to M_Z is shown in Figure 2. It is clear that all the masses decrease as we move from unification scale to low scale (cf. Figure 2). Initially, at unification scale, the splitting among the masses is relatively large but after RG evolution the splitting gets narrowed down and they acquire nearly degenerate mass at M_Z .

Low energy threshold corrections to neutrino masses

It is evident from table II that only one (i.e. Δm_{32}^2) out of two mass squared differences, at the low scale, lies within experimental $3\text{-}\sigma$ range. This discrepancy can easily be accounted for by threshold corrections [3, 5]. In the case of quasi-degenerate neutrinos, the low energy

¹ The RG evolution of θ_{13} and θ_{23} is correlated in the HSMU hypothesis. Therefore, at the low scale, both cannot be obtained near their best fit values simultaneously.

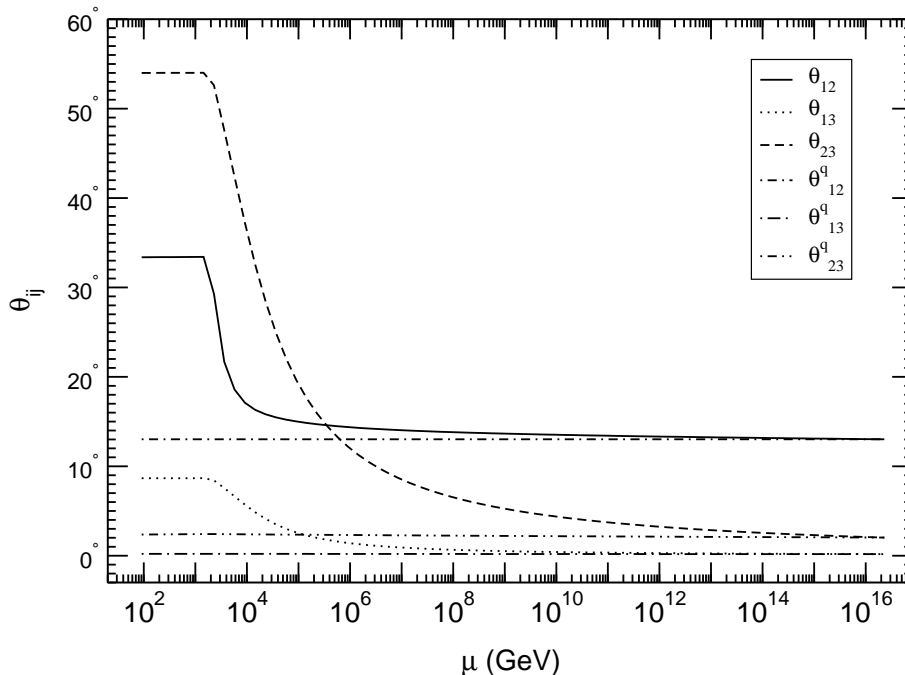


FIG. 1: The RG evolution of CKM and PMNS mixing angles with respect to RG scale (μ). This figure corresponds to the neutrino oscillation parameters quoted in the first column of Table II.

MSSM threshold corrections can result in a significant contribution, as shown in [29–32]. These threshold corrections are given by following equations [3, 5]:

$$\begin{aligned}
 (\Delta m_{21}^2)_{th} &= 2m^2 \cos 2\theta_{12}[-2T_e + T_\mu + T_\tau], \\
 (\Delta m_{32}^2)_{th} &= 2m^2 \sin^2 \theta_{12}[-2T_e + T_\mu + T_\tau], \\
 (\Delta m_{31}^2)_{th} &= 2m^2 \cos^2 \theta_{12}[-2T_e + T_\mu + T_\tau].
 \end{aligned} \tag{7}$$

Here, $m = \frac{1}{3}(m_1 + m_2 + m_3)$ is the mean mass of the quasi-degenerate neutrinos and T_α ($\alpha = e, \mu, \tau$) is the one-loop factor. Its form has been previously calculated in [29, 32] and given by

$$T_\alpha = \frac{g_2^2}{32\pi^2} \left[\frac{x_\mu^2 - x_\alpha^2}{y_\mu y_\alpha} + \frac{(y_\alpha^2 - 1)}{y_\alpha^2} \ln(x_\alpha^2) - \frac{(y_\mu^2 - 1)}{y_\mu^2} \ln(x_\mu^2) \right], \tag{8}$$

where g_2 is the $SU(2)$ coupling constant and $y_\alpha = 1 - x_\alpha^2$ with $x_\alpha = M_\alpha/M_{\tilde{w}}$; $M_{\tilde{w}}$ stands for wino mass, M_α represents the mass of charged sleptons. Moreover, without any loss of generality, the loop-factor has been defined to give $T_\mu = 0$ (cf. [3, 5] for details).

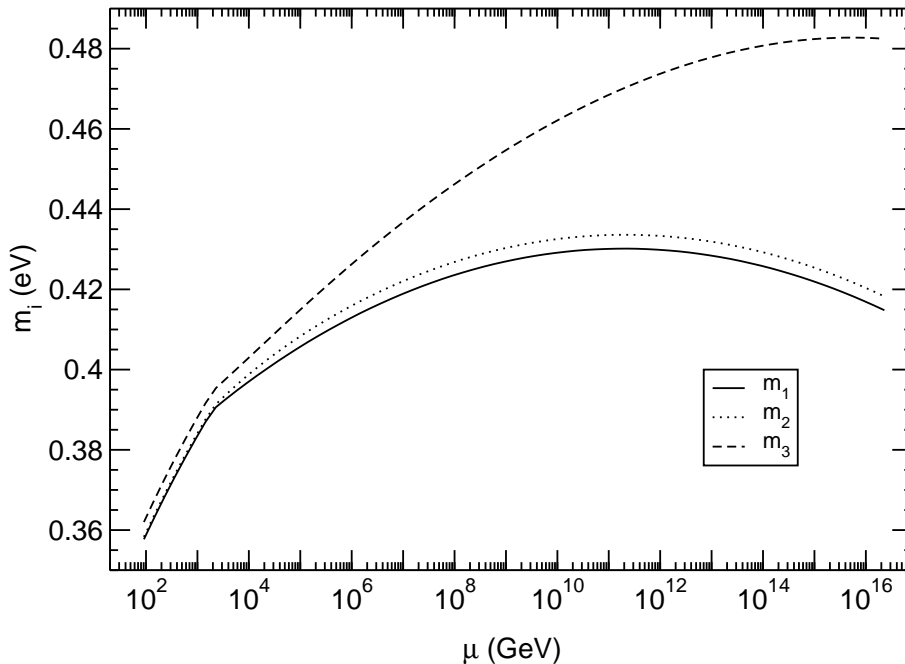


FIG. 2: The RG evolution of neutrino masses (m_i) with respect to RG scale (μ). This figure corresponds to the values in the first column of Table II.

At the LHC, for simplified scenarios, chargino masses are excluded up to 750 GeV in the presence of light sleptons and up to 300 GeV in the case of heavy sleptons [17, 18]. In the view of above constraints, here we have taken the wino mass to be 800 GeV.

After the inclusion of threshold corrections, along with the RG-evolution effects, the final expression for mass squared differences is given as

$$\Delta m_{ij}^2 = (\Delta m_{ij}^2)_{\text{RG}} + (\Delta m_{ij}^2)_{\text{th}}. \quad (9)$$

It is clear from table II, that the RG effects, along with threshold corrections, result in good agreement between the predictions of HSMU hypothesis and the present experimentally allowed range of neutrino oscillation parameters (cf. Table I). At this juncture, we would like to point out that, although the threshold corrections for mass square differences are significant yet they are negligibly small compare to the mean mass of neutrinos. The same is also true for the threshold corrections to mixing angles [3, 5].

IV. PREDICTIONS FROM HSMU HYPOTHESIS

Within the framework of the HSMU hypothesis, the low energy oscillation data can be used to put stringent constraints on the allowed parameter range for the neutrino masses and mixing angle. The aim of this section is to discuss the predictions from our analysis which are obtained after imposing these constraints. These predictions can be tested in present and future experiments as discussed in this section.

A. Predictions for Masses, $\langle M_\beta \rangle$ and $\langle M_{\beta\beta} \rangle$ at M_Z

As clear from Table II, the neutrino masses at M_Z lie in the range of 0.34-0.38 eV. This range can be probed by various presently running as well as near future experiments and hence it provides an important test for HSMU hypothesis. For example, the recent result from GERDA gives an upper bound of 0.2-0.4 eV on the $\langle M_{\beta\beta} \rangle$ component of mass matrix [33]. Similarly, EXO-200 provides an upper bound of 0.14-0.38 eV on the same [34]. Although the present bounds on $\langle M_\beta \rangle$ from tritium beta decay are comparatively weak (< 2 eV) [35–37]. In future, the KATRIN experiment will be able to probe it down to 0.2 eV [38].

Moreover, the recent Planck data has provided a bound on the sum of neutrino masses in the range of 0.23-1.08 eV depending on the choice of the priors [39]. The lower limit of Planck is in tension with our hypothesis but it should be noted that the cosmological constraints are highly model dependent and should be taken in conjunction with other experiments. In view of the above considerations, the absolute value of neutrino masses provides an important test of our hypothesis. We would like to point out that the above mentioned mass range (0.34-0.38 eV) is obtained for a specific choice of unification scale, SUSY breaking scale and $\tan\beta$ (cf. Table II for details). The dependence of neutrino masses (at M_Z) with respect to these parameters is discussed, in detail, in section V.

B. Predictions for mixing angles at M_Z

It is clear from the RG equations (5) that, within HSMU hypothesis, the mixing angles θ_{13} and θ_{23} are correlated. In Figure 3, we show the explicit dependence of θ_{23} on θ_{13} keeping other low scale neutrino oscillation parameters fixed near to their best fit values. We observe

that θ_{23} turns out to be above 45° (i.e. lies in the second octant), for the whole $3\text{-}\sigma$ range of θ_{13} . This prediction is easily testable in the current and in future experiments, like INO, T2K, NO ν A, LBNE, Hyper-K and PINGU [40–45].

Even for the lower edge value of the present $3\text{-}\sigma$ range of θ_{13} , the value of θ_{23} is non-maximal and is around 47° , as evident from Figure 3. The values of θ_{23} increase with θ_{13} . When θ_{13} is around 9° , θ_{23} reaches its upper edge of $3\text{-}\sigma$ limit and it goes into the disfavored region for higher values of θ_{13} (which is still within its $3\text{-}\sigma$ range). This, in turn, puts constraints on the values of θ_{13} , which should lie in the range $7.19^\circ\text{--}8.8^\circ$.

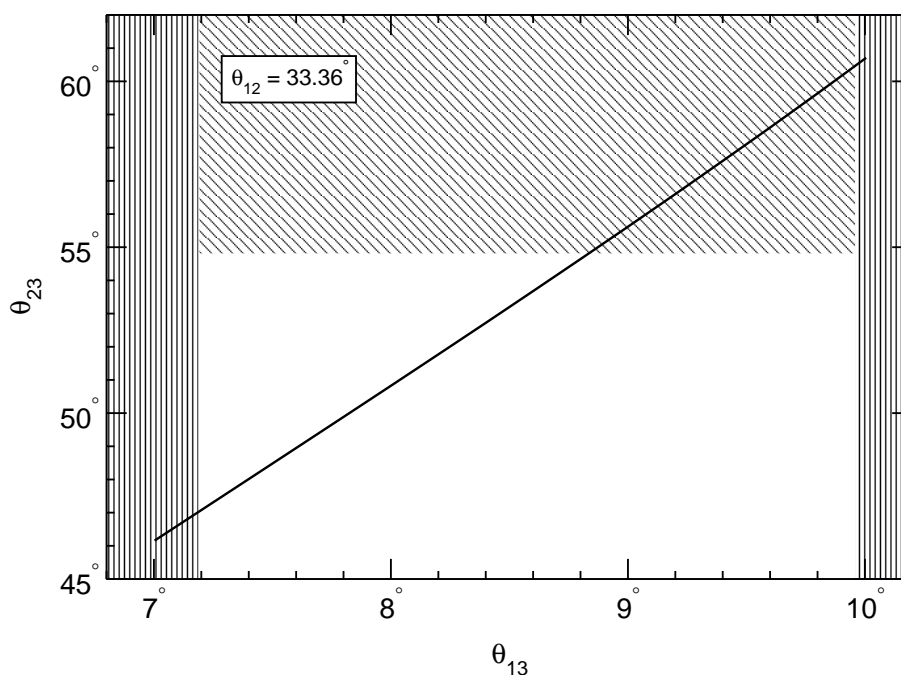


FIG. 3: The variation of θ_{23} with respect to θ_{13} . For plotting this figure we have kept all other oscillation parameters to be at their best-fit values. The vertically shaded regions lie outside the $3\text{-}\sigma$ range of θ_{13} whereas the horizontally shaded one lies outside $3\text{-}\sigma$ range of θ_{23} [14].

At this point we would like to mention that, the RG evolution of θ_{12} also depends on Δm_{21}^2 . Therefore, it can be varied independently of the other two angles by making an appropriate

² As shown in table II, θ_{23} also depends very weakly on θ_{12} . The above quoted range is for θ_{12} at its best fit value.

choice of Δm_{21}^2 at unification scale. Hence, within HSMU hypothesis, no effective constraints on its range can be obtained.

V. ALLOWED PARAMETER RANGE FOR UNIFICATION SCALE, SUSY BREAKING SCALE AND $\tan \beta$

In this section, we study the variation of unification scale, SUSY breaking scale and $\tan \beta$ and its impact on HSMU hypothesis. We derive constraints on the range of these parameters for which HSMU hypothesis works. For this purpose, in this section, we have fixed the values of experimentally measured quantities θ_{12} and θ_{13} to their best fit values (i.e. 33.36° and 8.66° respectively) at M_Z . We also fix $\Delta m_{32}^2 = 2.5 \times 10^{-3} \text{eV}^2$, which is slightly higher than its best fit value, so that after adding appropriate threshold corrections, it remains within $3\text{-}\sigma$ range.

Since in our hypothesis the quantities θ_{23} and Δm_{21}^2 are fixed in terms of other quantities, we have not put any restrictions on them, apart from the fact that, after adding appropriate threshold corrections they should remain within $3\text{-}\sigma$ limit.

A. Variation of Unification Scale

In the previous sections, we have chosen our unification scale as 2×10^{16} GeV which is the typical scale for GUTs. Since our hypothesis does not depend on the details of the high scale theory, it is not necessary to take the unification scale to be same as that of GUT. Thus, in this subsection, we analyze the effect of variation of unification scale.

It is clear from Figure 1, that a major part of angle magnification happens only close to M_{SUSY} . Therefore, it is expected that the desired angle magnification can be achieved even when the unification scale is not same as the GUT scale. In Figure 4 and 5, we have, respectively, shown the variation of unification scale with respect to high and low scale neutrino masses. The magnitude of low scale masses (and derived quantities such as $\langle M_\beta \rangle$ and $\langle M_{\beta\beta} \rangle$) put constraints³ on the unification scale as evident from the Figure 5 and further

³ In our case, since the neutrinos are quasi-degenerate and phases are absent, the mean mass (m) and $\langle M_{\beta\beta} \rangle$ are almost the same. Hence, in drawing the constraints in Figures 5, 7 and 9 we have neglected the small difference in the exact values of m and $\langle M_{\beta\beta} \rangle$.

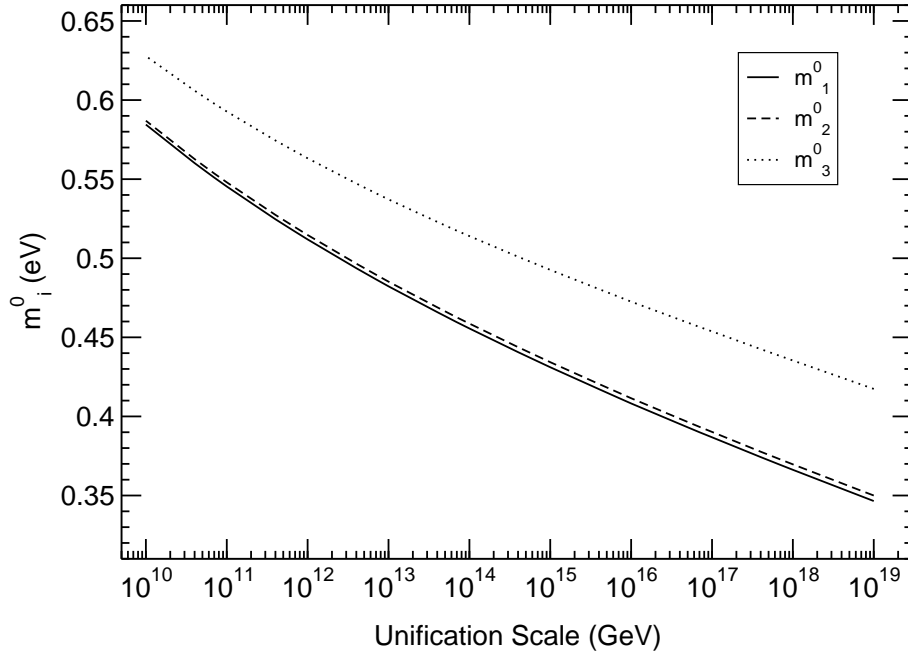


FIG. 4: Unification scale vs neutrino masses (m_i^0) at unification scale. In plotting this figure we have taken $M_{SUSY} = 2 \times 10^3$ GeV and $\tan \beta = 55$.

elaborated in Section V D.

Our analysis works for a wide range of unification scale from the Planck scale to much lower scales (cf. Figures 4, 5). The reason for this is that the major part of magnification of angles happens in a relatively small range near M_{SUSY} . Hence, one can take the unification scale to be several orders of magnitude lower than the GUT scale and still achieve desired magnification at M_Z . The noteworthy point is that as we lower the unification scale the input neutrino masses have to be taken more degenerate because the range of MSSM RG running becomes shorter (cf. Figure 4). Thus, to achieve desired magnifications at M_Z , one has to make the input neutrino masses more degenerate to account for the lesser range of MSSM RG running.

This increasing degeneracy of masses, in turn, results in Δm_{32}^2 approaching its $3\text{-}\sigma$ range much before M_Z . Therefore, to counter this and to keep Δm_{32}^2 within its $3\text{-}\sigma$ range at M_Z , one is also forced to increase the mean input mass at unification scale. Furthermore, once the input mean mass is increased, it results in a relative increase in the mean mass at M_Z ,

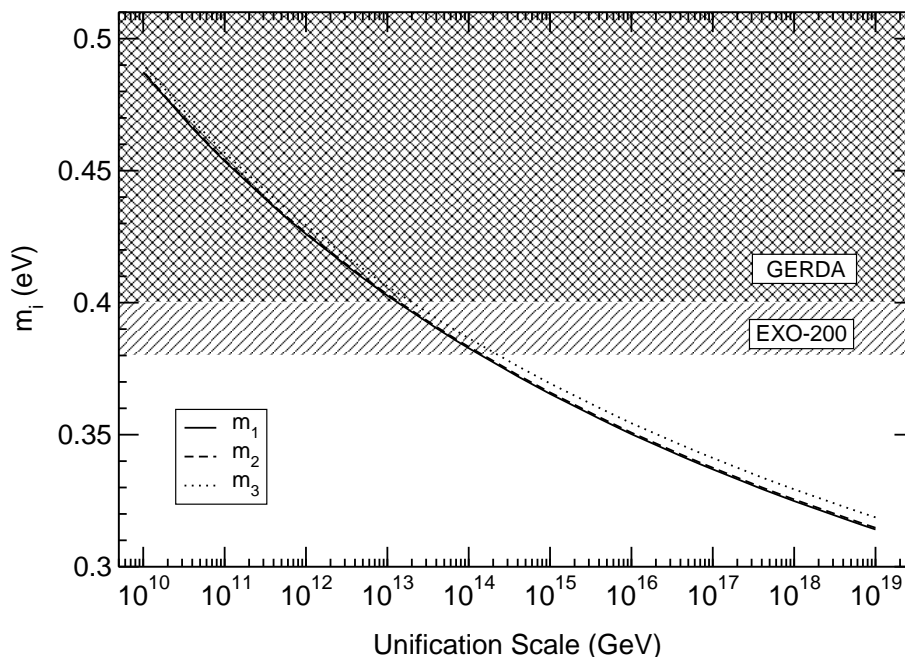


FIG. 5: Unification scale vs neutrino masses (m_i) at M_Z . Here we have taken $M_{SUSY} = 2 \times 10^3$ GeV and $\tan \beta = 55$. The shaded regions are excluded by $0\nu\beta\beta$ decay experiments [33, 34].

partly because now it is higher to begin with and partly because of the small range of MSSM RG running.

Thus, the mean mass of neutrinos at unification scale as well as at M_Z increases as we decrease the unification scale. Hence, one can constrain the lowest possible unification scale using data from various experiments. We will further elaborate on such experimental constraints in Section VD.

B. Variation of SUSY Breaking Scale

We have, so far, fixed the SUSY breaking scale at 2×10^3 GeV. In this section, we analyze the effects of variation of SUSY breaking scale. It is clear from Figure 1 that the major part of magnification occurs only in and around the SUSY breaking scale. So one should expect to shift the scale of SUSY breaking from the so far chosen value and still be able to achieve the desired magnification. Our analysis works for a wide range of SUSY breaking

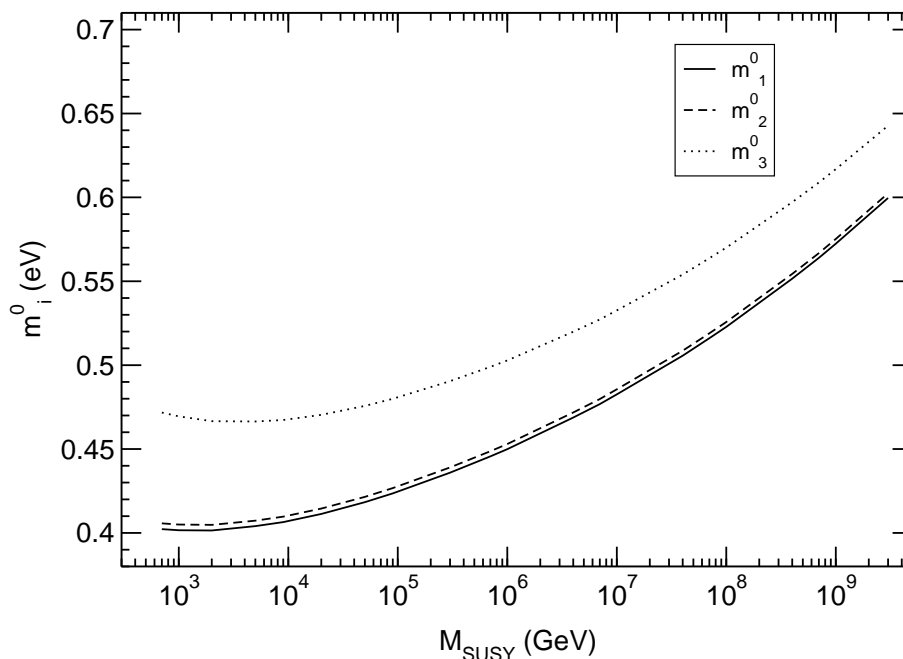


FIG. 6: M_{SUSY} vs neutrino masses (m_i^0) at unification scale. In plotting this figure, we have taken unification scale = 2×10^{16} GeV and $\tan\beta = 55$.

scale starting from the TeV scale to much higher scales (as is clear from Figures 6 and 7). While plotting these figures, we have taken the unification scale = 2×10^{16} GeV, $\tan\beta = 55$ and the value of observables at M_Z to be same as before.

As we increase the SUSY breaking scale, the input neutrino masses have to be taken to be more degenerate. The reason for this is that by increasing the SUSY breaking scale the range of MSSM RG running becomes shorter. Thus, to achieve desired magnifications at M_Z one has to make the input neutrino masses more degenerate in order to counter the lesser range of MSSM RG running. At the same time, we have to increase the mean mass of neutrinos at unification scale in order to keep the Δm_{32}^2 within its $3\text{-}\sigma$ range at M_Z .

Since the mean mass of the neutrinos increases with increasing SUSY breaking scale, one can constrain the highest possible SUSY breaking scale using data from various experiments. Moreover, the lower ranges of SUSY breaking scale are constrained from SUSY searches at the LHC [17, 18]. We further discuss these constraints in the Section VD.

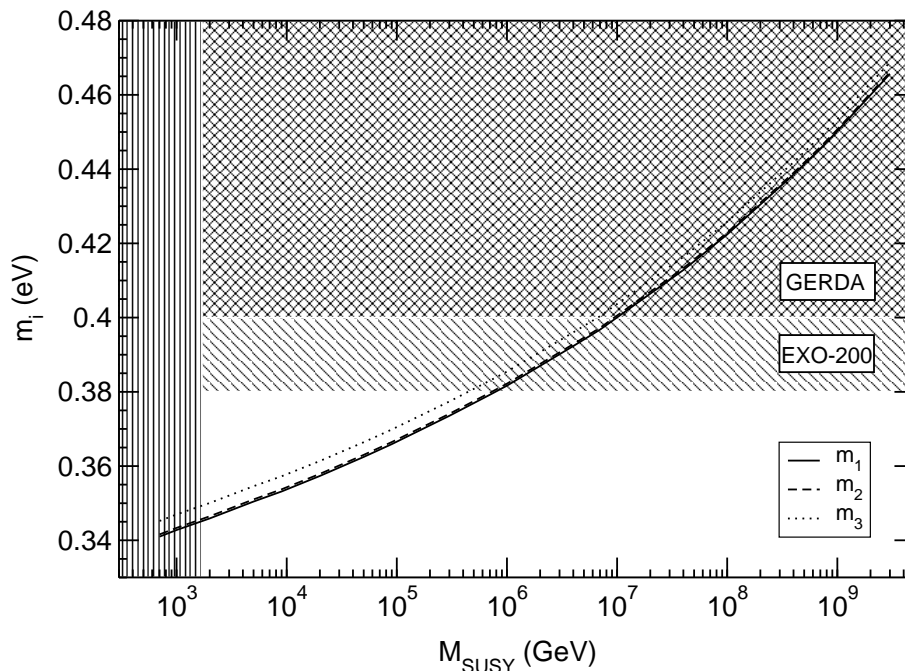


FIG. 7: M_{SUSY} vs neutrino masses (m_i) at M_Z . In plotting this figure, we have taken unification scale = 2×10^{16} GeV and $\tan \beta = 55$. The vertically shaded region is disfavored by the LHC SUSY searches [18] whereas the horizontal ones are excluded by $0\nu\beta\beta$ decay experiments [33, 34].

C. Variation of $\tan \beta$

In MSSM, the RG running of angles gets enhanced by a factor of $(1 + \tan^2 \beta)$ [cf. (5) for details]. Therefore, the larger values of $\tan \beta$ enhance the magnification at M_Z . This is the reason for choosing $\tan \beta = 55$ in the previous sections of this work. We have, so far, fixed $\tan \beta = 55$ but in this section we will vary $\tan \beta$ to obtain the lower limits on it for desired magnification.

It is clear from Figures 8 and 9 that the mixing angle magnification happens for a wide range of $\tan \beta$. Although we have not shown this in the figure, the desired angle magnifications can be obtained for values of $\tan \beta$ as low as 4 or 5. But, for low $\tan \beta$ the masses of neutrinos become very high at low scale. Furthermore, if we take low values of $\tan \beta$, the input neutrino masses, at unification scale, have to be taken more degenerate and the mean

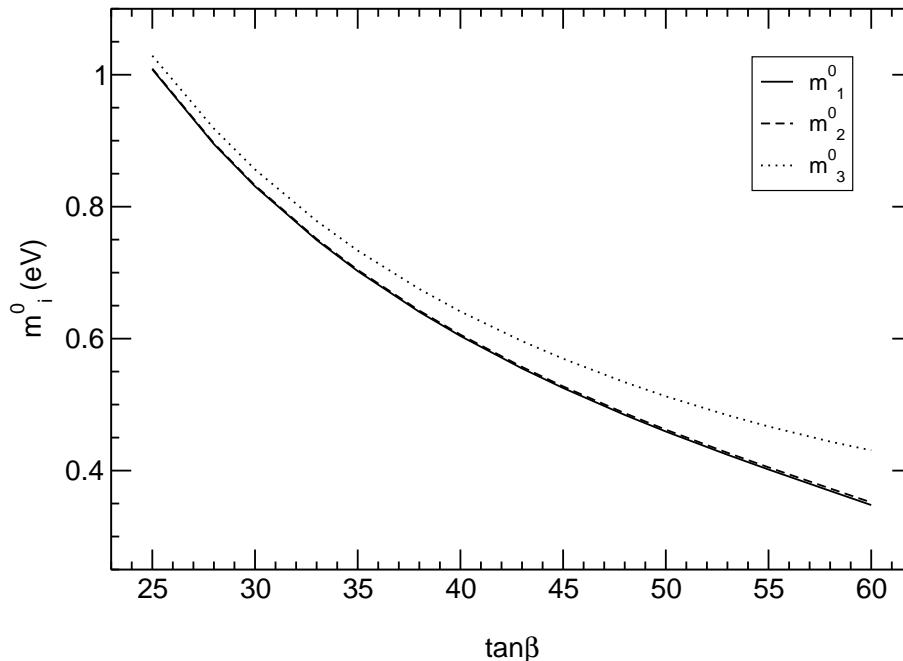


FIG. 8: Variation of $\tan\beta$ vs neutrino masses (m_i^0) at unification scale. In plotting this figure, we have taken unification scale = 2×10^{16} GeV and $M_{SUSY} = 2 \times 10^3$ GeV.

mass should also be higher. The reason is that with decreasing $\tan\beta$ the factor $(1 + \tan^2\beta)$ becomes small. Thus, to achieve desired magnifications at M_Z one has to make the input neutrino masses more degenerate to account for the smaller contribution coming from $(1 + \tan^2\beta)$ term. At the same time to keep Δm_{32}^2 within its $3\text{-}\sigma$ range at M_Z , one is forced to increase the mean input mass at unification scale. Since the mean mass of the neutrinos increases with decreasing $\tan\beta$, one can constrain the range of allowed $\tan\beta$ from various experiments, as discussed in Section V D.

D. Experimental Constraints

As is clear from previous discussion, the mean mass of neutrinos varies with the variation of the unification scale, SUSY breaking scale and $\tan\beta$. Therefore, one can constrain the range of these parameters by using data from various experiments, as discussed below.

(i) *Constraints from Tritium Beta Decay:* The present constraints on $\langle m_\beta \rangle$ coming from tritium beta decay are $\langle m_\beta \rangle < 2$ eV [35–37]. They give only the upper bound on the masses

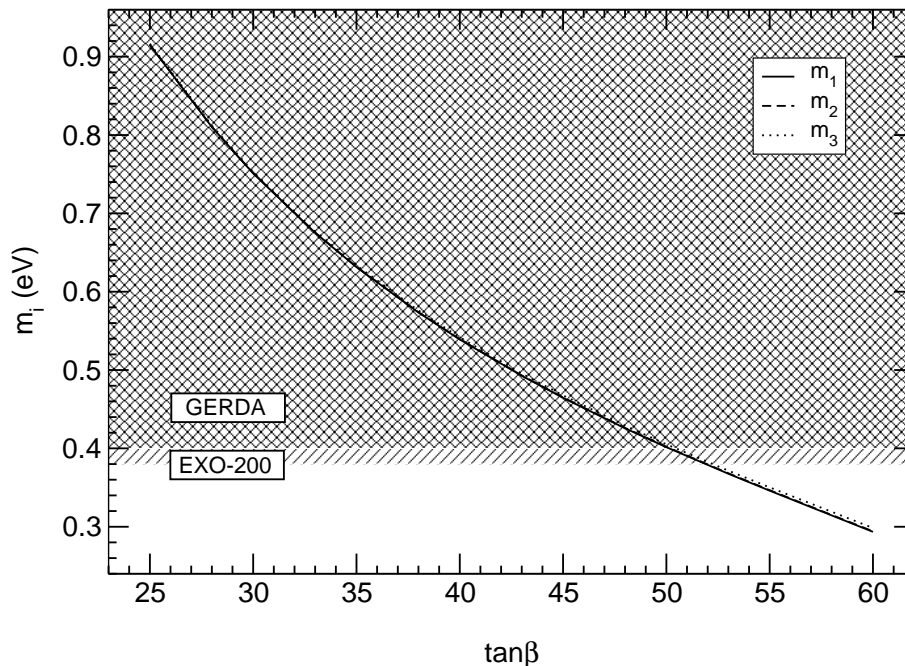


FIG. 9: Variation of $\tan\beta$ vs neutrino masses (m_i) at M_Z . In plotting this figure, we have taken unification scale = 2×10^{16} GeV and $M_{SUSY} = 2 \times 10^3$ GeV. The shaded regions are excluded by $0\nu\beta\beta$ decay experiments [33, 34].

of the neutrinos and thus the whole mass range of the Figures 5, 7 and 9 easily comes under this limit. Hence, the tritium beta decay constraints are relatively weak. They allow much lower values of the unification scale, $\tan\beta$ and much higher values of SUSY breaking scale than those plotted in the above figures. However, in future, the KATRIN experiment is expected to probe $\langle m_\beta \rangle$ as low as 0.2 eV [38] and hence will be able to put much tighter constraints on the allowed range of these parameters.

(ii) *Constraints from Neutrinoless Double Beta Decay:* At present, the EXO-200 and GERDA experiments provide the most stringent constraints on $\langle m_{\beta\beta} \rangle$. The latest results from phase I of the GERDA experiment have given the upper limit on $\langle m_{\beta\beta} \rangle$ to be 0.20-0.40 eV [33], whereas EXO-200 has given an upper limit of 0.14-0.38 eV [34]. This, in turn, puts stringent constraints on the allowed range of various parameters, as given below.

(a) The lower limit of unification scale is constrained to be around 10^{13} GeV by GERDA and around 10^{14} GeV by EXO-200 (cf. Figure 5).

(b) The results from GERDA constrains the highest possible SUSY breaking scale to be

around 10^7 GeV, whereas EXO-200 puts a limit of around 10^6 GeV (cf. Figure 7).

(c) The lowest possible value of $\tan\beta$ is constrained to be around 50 (cf. Figure 9).

In future, these limits are expected to improve, thus resulting in more tighter constraints e.g. the GERDA phase II is aiming for an increased sensitivity by a factor of about 10 (cf. [33] for details). It should be noted that the above constraints are for the case when all the PMNS phases are taken to be zero. These constraints are likely to change in the presence of phases. We will analyze them, in detail, in our next work [24].

(iii) *Cosmological Constraints:* The recent result of the Planck collaboration has given constraints on the sum of neutrino masses to be in the range of 0.23 eV [95%; Planck+WP+highL+BAO] to 1.08 eV [95%; Planck+WP+highL (A_L)] depending on values chosen for the priors [39]. The limit of 1.08 eV implies that the mean neutrino mass has to be around 0.36 eV, thus putting similar constraints to those obtained from $\langle m_{\beta\beta} \rangle$. The lowest value (i.e. 0.23 eV [95%; Planck+WP+highL+BAO]) is in tension with our hypothesis. However, as noted by the Planck collaboration itself, the cosmological limits are highly dependent on chosen values of priors, so these limits should be taken as indicative and not conclusive.

To conclude, in view of the above experimental constraints, for fixed values of other parameters, (1) The unification scale should be taken around 10^{14} GeV or above, (2) The SUSY breaking scale should be taken below 10^6 GeV and (3) The $\tan\beta$ should be taken above 50.

VI. CONCLUSIONS

We have investigated the implications of High Scale Mixing Unification hypothesis in the wake of new data and experimental constraints. This hypothesis leads to the experimentally observed mixing angles and mass square differences at low energy scales (M_Z). The small but non-zero value of θ_{13} is a natural outcome of this hypothesis which has been recently confirmed by various experiments [8–12]. We found that, in absence of phases, for the present $3\text{-}\sigma$ range of θ_{13} HSMU hypothesis uniquely predicts the value of θ_{23} to be non-maximal and above 45° . The normal hierarchy and quasi-degeneracy of neutrino masses are essential assumptions to realize HSMU hypothesis. We have also analyzed the allowed parameter range for other parameters of our hypothesis *vis-a-vis* various experimental constraints. We

found that (i) the unification scale should be above 10^{14} GeV, (ii) the SUSY breaking scale should lie below 10^6 GeV, and (iii) the value of $\tan\beta$ should be taken above 50.

However, it should be noted that all the above conclusions have been drawn by taking Dirac as well as Majorana phases of PMNS matrix to be zero. These conclusions may change in the presence of phases. The detailed implications of these phases are under investigation and will be reported in our future publications [24].

Moreover, in a recent analysis of the HSMU hypothesis with Dirac type neutrinos, we have found similar predictions for mixing angles [6]. At the end, we would like to point out that the above mentioned two scenarios can be distinguished from each other by the scale of their mean mass (or $\langle m_\beta \rangle$) and $\langle m_{\beta\beta} \rangle$ measurements.

Acknowledgments

We would like to thank R. N. Mohapatra, M. K. Parida, S. K. Agarwalla, M. Hirsch and A. Pich for their useful comments and suggestions. RS would also like to thank A. Menon, R. Laha and S. Vempati for their valuable comments and suggestions.

-
- [1] R. N. Mohapatra, M. K. Parida and G. Rajasekaran, Phys. Rev. D **69**, 053007 (2004) [hep-ph/0301234].
 - [2] R. N. Mohapatra, M. K. Parida and G. Rajasekaran, Pramana **62**, 643 (2004).
 - [3] R. N. Mohapatra, M. K. Parida and G. Rajasekaran, Phys. Rev. D **71**, 057301 (2005) [hep-ph/0501275].
 - [4] R. N. Mohapatra, M. K. Parida and G. Rajasekaran, Phys. Rev. D **72**, 013002 (2005) [hep-ph/0504236].
 - [5] S. K. Agarwalla, M. K. Parida, R. N. Mohapatra and G. Rajasekaran, Phys. Rev. D **75**, 033007 (2007) [hep-ph/0611225].
 - [6] G. Abbas, S. Gupta, G. Rajasekaran and R. Srivastava, arXiv:1312.7384 [hep-ph].
 - [7] N. Haba and R. Takahashi, Europhys. Lett. **100**, 31001 (2012) [arXiv:1206.2793 [hep-ph]].
 - [8] K. Abe *et al.* [T2K Collaboration], Phys. Rev. Lett. **107**, 041801 (2011) [arXiv:1106.2822 [hep-ex]].

- [9] P. Adamson *et al.* [MINOS Collaboration], Phys. Rev. Lett. **107**, 181802 (2011) [arXiv:1108.0015 [hep-ex]].
- [10] Y. Abe *et al.* [Double Chooz Collaboration], Phys. Rev. D **86**, 052008 (2012) [arXiv:1207.6632 [hep-ex]].
- [11] J. K. Ahn *et al.* [RENO Collaboration], Phys. Rev. Lett. **108**, 191802 (2012) [arXiv:1204.0626 [hep-ex]].
- [12] F. P. An *et al.* [DAYA-BAY Collaboration], Phys. Rev. Lett. **108**, 171803 (2012) [arXiv:1203.1669 [hep-ex]].
- [13] G. L. Fogli, E. Lisi, A. Marrone, D. Montanino, A. Palazzo and A. M. Rotunno, Phys. Rev. D **86**, 013012 (2012) [arXiv:1205.5254 [hep-ph]].
- [14] M. C. Gonzalez-Garcia, M. Maltoni, J. Salvado and T. Schwetz, JHEP **1212**, 123 (2012) [arXiv:1209.3023 [hep-ph]].
- [15] G. Aad *et al.* [ATLAS Collaboration], Phys. Lett. B **716**, 1 (2012) [arXiv:1207.7214 [hep-ex]].
- [16] S. Chatrchyan *et al.* [CMS Collaboration], Phys. Lett. B **716**, 30 (2012) [arXiv:1207.7235 [hep-ex]].
- [17] <https://twiki.cern.ch/twiki/bin/view/AtlasPublic/SupersymmetryPublicResults>,
<https://twiki.cern.ch/twiki/bin/view/CMSPublic/PhysicsResultsSUS>.
- [18] N. Craig, arXiv:1309.0528 [hep-ph].
- [19] W. Altmannshofer, M. Carena, N. R. Shah and F. Yu, JHEP **1301**, 160 (2013) [arXiv:1211.1976 [hep-ph]].
- [20] S. Antusch, J. Kersten, M. Lindner, M. Ratz and M. A. Schmidt, JHEP **0503**, 024 (2005) [hep-ph/0501272].
- [21] S. Antusch and M. Ratz, JHEP **0207**, 059 (2002) [hep-ph/0203027].
- [22] J. A. Casas, J. R. Espinosa, A. Ibarra and I. Navarro, Nucl. Phys. B **573**, 652 (2000) [hep-ph/9910420].
- [23] S. Antusch, J. Kersten, M. Lindner and M. Ratz, Nucl. Phys. B **674**, 401 (2003) [hep-ph/0305273].
- [24] S. Gupta, G. Rajasekaran and R. Srivastava (work under preparation).
- [25] Z. -z. Xing, H. Zhang and S. Zhou, Phys. Rev. D **86**, 013013 (2012) [arXiv:1112.3112 [hep-ph]].
- [26] C. Beskidt, W. de Boer and D. I. Kazakov, arXiv:1308.1333 [hep-ph].
- [27] A. Abada, A. J. R. Figueiredo, J. C. Romao and A. M. Teixeira, JHEP **1208**, 138 (2012)

- [arXiv:1206.2306 [hep-ph]].
- [28] M. Hirsch, F. R. Joaquim and A. Vicente, JHEP **1211**, 105 (2012) [arXiv:1207.6635 [hep-ph]].
- [29] E. J. Chun and S. Pokorski, Phys. Rev. D **62**, 053001 (2000) [hep-ph/9912210].
- [30] P. H. Chankowski, A. Ioannisian, S. Pokorski and J. W. FValle, Phys. Rev. Lett. **86**, 3488 (2001) [hep-ph/0011150].
- [31] E. J. Chun, Phys. Lett. B **505**, 155 (2001) [hep-ph/0101170].
- [32] P. H. Chankowski and P. Wasowicz, Eur. Phys. J. C **23**, 249 (2002) [hep-ph/0110237].
- [33] M. Agostini *et al.* [GERDA Collaboration], Phys. Rev. Lett. **111**, 122503 (2013) [arXiv:1307.4720 [nucl-ex]].
- [34] M. Auger *et al.* [EXO Collaboration], Phys. Rev. Lett. **109**, 032505 (2012) [arXiv:1205.5608 [hep-ex]].
- [35] Ch. Kraus, B. Bornschein, L. Bornschein, J. Bonn, B. Flatt, A. Kovalik, B. Ostrick and E. W. Otten *et al.*, Eur. Phys. J. C **40**, 447 (2005) [hep-ex/0412056].
- [36] V. N. Aseev *et al.* [Troitsk Collaboration], Phys. Rev. D **84**, 112003 (2011) [arXiv:1108.5034 [hep-ex]].
- [37] J. Beringer *et al.* [Particle Data Group Collaboration], Phys. Rev. D **86**, 010001 (2012).
- [38] G. Drexlin, V. Hannen, S. Mertens and C. Weinheimer, Adv. High Energy Phys. **2013**, 293986 (2013) [arXiv:1307.0101 [physics.ins-det]].
- [39] P. A. R. Ade *et al.* [Planck Collaboration], arXiv:1303.5076 [astro-ph.CO].
- [40] M. S. Athar *et al.* [INO Collaboration], INO-2006-01.
- [41] K. Abe *et al.* [T2K Collaboration], Nucl. Instrum. Meth. A **659**, 106 (2011), arXiv:1106.1238.
- [42] R. B. Patterson [NOvA Collaboration], Nucl. Phys. Proc. Suppl. **235-236**, 151 (2013), arXiv:1209.0716.
- [43] C. Adams *et al.* [LBNE Collaboration], arXiv:1307.7335.
- [44] E. Kearns *et al.* [Hyper-Kamiokande Working Group Collaboration], arXiv:1309.0184.
- [45] S. -F. Ge and K. Hagiwara, arXiv:1312.0457.